

# Introduction to high- $p_T$ inclusives

Matthew Wing<sup>†</sup>

<sup>†</sup>*McGill University, Physics Department,  
3600 University Street, Montreal,  
Canada, H3A 2T8  
E-mail: wing@mail.desy.de*

**Abstract.** A selection of theoretical and experimental results are presented in the broader context of understanding QCD and its relation to photon physics. A phenomenological analysis of HERA data to constrain the gluon content of the proton and photon is discussed. Measurements from the Tevatron and fixed-target experiments are compared to theoretical predictions. Finally, the future of higher order pQCD calculations is addressed.

## INTRODUCTION

In these proceedings, advances in understanding QCD are discussed in experiments which directly complement those where measurements of the photon structure are being made. For a generalised accelerator, where the incoming particles,  $I_1$  and  $I_2$  resolve into partons, the cross section at leading order,  $d\sigma_{I_1 I_2 \rightarrow cd}$ , can be written as,

$$d\sigma_{I_1 I_2 \rightarrow cd} = \sum_{ab} \int_{x_{I_2}} \int_{x_{I_1}} f_{I_2 \rightarrow b}(x_{I_2}, \mu_{I_2}^2) f_{I_1 \rightarrow a}(x_{I_1}, \mu_{I_1}^2) \mathcal{M}_{ab \rightarrow cd}^2, \quad (1)$$

where  $f_{I \rightarrow b}(x_I, \mu_I^2)$ , is the parton density function for a give momentum fraction,  $x_I$  and factorisation scale,  $\mu_I$  and  $\mathcal{M}_{ab \rightarrow cd}$  is the  $2 \rightarrow 2$  matrix element. This entails two or three unknowns; the perturbatively calculable matrix element and one or two structure functions. From equation (1) it can be seen that other experiments, such as the Tevatron, can provide complementary information on  $\mathcal{M}_{ab \rightarrow cd}$  and therefore indirectly help measurements of the photon structure function.

## HERA PHOTOPRODUCTION DATA

Improvements in the understanding of pQCD for jet photoproduction have led to the agreement between independent calculations to within 5 – 10% [1,2]. Considering the cross section as a function of pseudorapidity of one jet whilst restricting

the other jet in the dijet system to a smaller region in pseudorapidity provides a good test of dijet production and the structure of the photon [1].

In a recent paper [3], Aurenche et al. have considered using the HERA photoproduction data to constrain the gluon content of the photon and proton. The distribution in  $x_\gamma^{\text{obs}}$ , the fraction of the photon's energy participating in the production of the two highest energy jets;

$$x_\gamma^{\text{obs}} = \frac{\sum_{\text{jet}1,2} E_T^{\text{jet}} e^{-\eta^{\text{jet}}}}{2yE_e}, \quad (2)$$

where  $yE_e$  is the initial photon energy, was considered in different regions of pseudorapidity of the jet. Requiring two jets,  $E_T^{\text{jet}1,2} > 12, 10$  GeV and the pseudorapidity,  $0 < \eta^{\text{jet}} < 1$ , the cross section shows a small dependence on the gluon distribution in the photon. However, when the jets are constrained to be more forward in pseudorapidity,  $1 < \eta^{\text{jet}} < 2$ , a significant sensitivity is seen at low- $x_\gamma^{\text{obs}}$ . A change of 30% in the gluon density of the photon results in a 25% change in the cross section at  $x_\gamma^{\text{obs}} = 0.2$ .

The NLO predictions are then compared to published data from the ZEUS collaboration [1], in which two jets,  $E_T^{\text{jet}1,2} > 14, 11$  GeV, are required to be within  $-1 < \eta^{\text{jet}} < 2$ . The comparison is shown in Figure 1, where one jet is restricted to be in the forward region,  $1 < \eta^{\text{jet}} < 2$  (Figure 1a) and the rear direction  $-1 < \eta^{\text{jet}} < 0$  (Figure 1b).

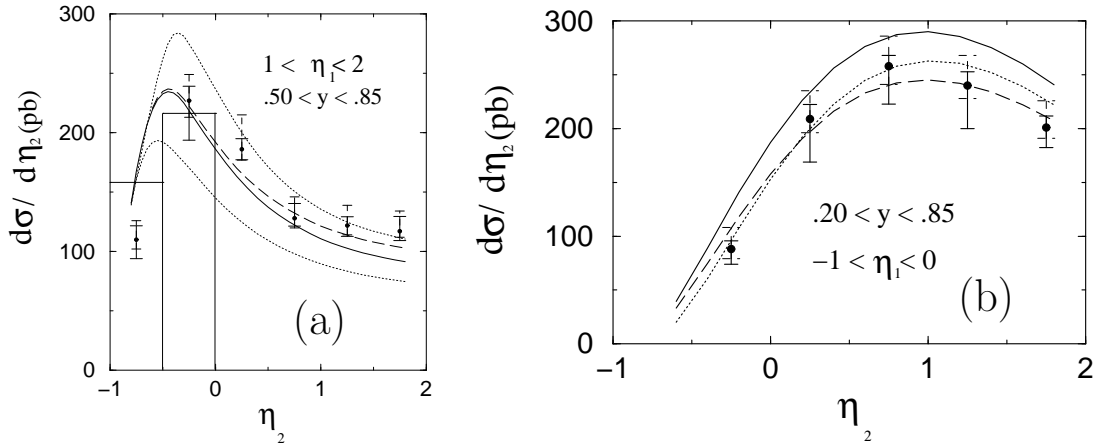


**FIGURE 1.** The NLO cross section  $d\sigma/d\eta_2$  compared to ZEUS data. In (a) the central prediction is the solid line and increasing the gluon content of the photon is the dashed line. In (b) the central prediction is the solid line and decreasing the gluon content of the proton is the dashed line. The dotted lines in (a) and (b) are changing the  $y$  distribution (from [3]).

In Figure 1a, increasing the gluon density in the photon by a value of 20% improves the description of the data at large values of  $\eta_2$ , increasing the cross section by  $\sim 10\%$ . At negative values of  $\eta_2$ , the prediction remains the same and is larger

than the data, however this region is subject to large hadronisation corrections. When the jet is in the rear direction as in Figure 1b, the cross section is less sensitive to the photon structure function and more so to the proton structure function. Decreasing the gluon density of the proton by 20% in this region improves the description of the data. However, it should again be noted that the hadronisation corrections increase with decreasing  $\eta_2$ .

Aurenche et al. conclude that the HERA data indicates a roughly 20% increase in the gluon content of the photon and a 20% decrease in the gluon content of the proton. The errors on the measurements are, however, as large as the change in cross section of these variations. Improved measurements are needed with larger statistics and are being investigated by both the H1 and ZEUS collaborations [4,5].

## TESTS OF QCD

Tests of QCD from other experiments, such as those at the Tevatron, complement those at HERA and LEP, with the Tevatron having the advantage of a better constrained incoming particle, the proton. Roughly, where HERA finishes;  $E_T^{\text{jet}} \sim 50$  GeV and  $M_{\text{jj}} \sim 200$  GeV, the Tevatron starts, providing overlap between the experiments at the different colliders. A selection of results of relevance to high- $E_T$  measurements at HERA and LEP will be discussed. In particular, high- $E_T$  jet production, jet substructure and prompt photon production will all be discussed later in the proceedings from at least one of the HERA or LEP experiments [6–8].

### High- $E_T$ jet production

Inclusive jet measurements at the Tevatron extend to values of  $E_T^{\text{jet}} \sim 450$  GeV [9], falling by  $\sim 7$  orders of magnitude as in Figure 2. The NLO prediction describes the data from the D0 collaboration very well, with the CDF data lying above the prediction at high transverse energies, which could be a signal for new physics such as quark substructure. However, the proton structure function is less well constrained at these large scales and the question of whether the data can be accommodated in a change of the proton PDF arises.

In Figure 3, the data is compared to the same calculation with three different proton structure functions. The MRST PDF gives a generally poor description of both the CDF and D0 measurements at low and high transverse energies. The CTEQ4M proton PDF gives a good description of the D0 data but inadequately describes the CDF data at high transverse energies. The CTEQ4HJ PDF includes the CDF data from Run IA in its fit, so would be expected to describe the Run IB data shown better than the other structure functions. This modified PDF describes well the D0 and the newer CDF data.

The comparison of data and theory clearly displays how understanding the parton density functions is essential in interpreting measurements in terms of new physics.

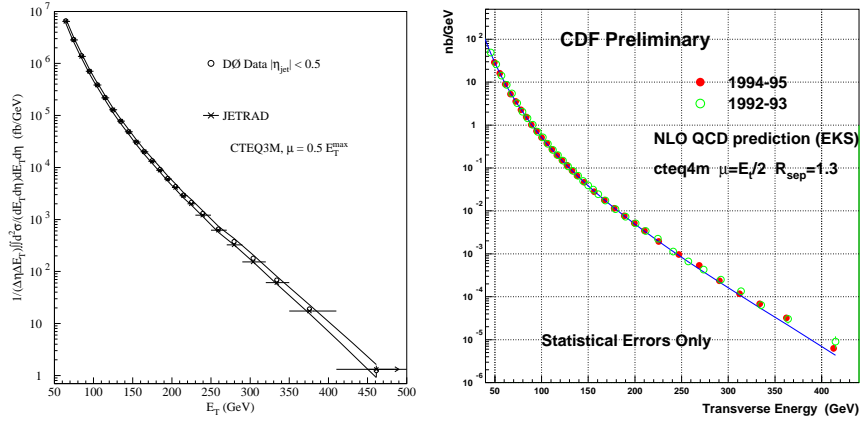


**FIGURE 2.** Inclusive jet cross sections from the (a) D0 (from [10]) and (b) CDF (from [11]) collaborations at  $\sqrt{s} = 1800$  GeV. The measurements are compared to NLO predictions.

Data to be and already analysed at HERA will allow the proton PDF to be further constrained at higher scales and hence more accurate predictions for the Tevatron measurements in Run II.

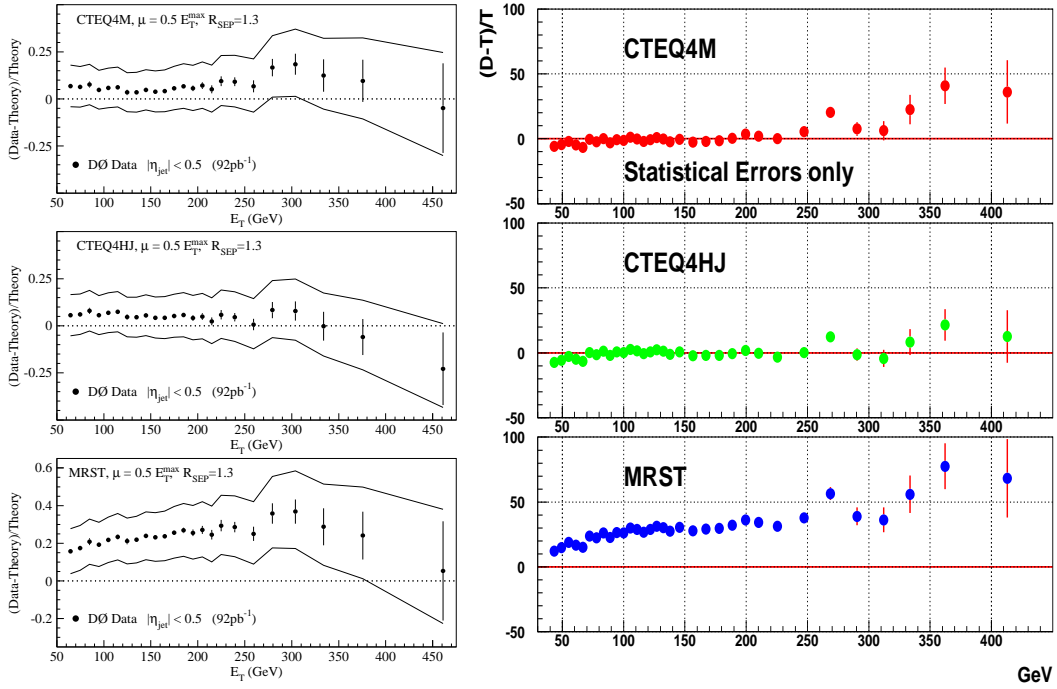


**FIGURE 3.** Relative difference of data and theory for inclusive jet cross sections from D0 [10] and CDF (from [11]) at  $\sqrt{s} = 1800$  GeV. The data is compared to three proton PDF's.

The Tevatron also produced data at centre-of-mass energies,  $\sqrt{s} = 630$  GeV, lower than the nominal  $\sqrt{s} = 1800$  GeV. Comparing the cross sections at the two

different energies provides a test of QCD whilst reducing systematic uncertainties on the measurement and the sensitivity to the choice of proton PDF. Figure 4a shows the ratio of the inclusive jet cross sections as a function of  $x_T \equiv \frac{2E_T}{\sqrt{s}}$  for both CDF and D0 data compared to NLO predictions. The reduction in the uncertainty in the choice of proton PDF can be seen in the difference of the prediction given by the three lines. At moderate and large  $x_T$ , the data agree well between the two collaborations, however at low  $x_T$ , the data sets diverge. At these lower values of  $x_T$ , the data suffer from possible problems of understanding the soft underlying event, which, both experiments correct for. The data also lie consistently below the prediction at the scale,  $\mu$ , chosen. Reasons for the discrepancy are unclear, with possible interpretations being the use of different renormalisation scales or  $k_T$  effects, although neither of these are attractive explanations.

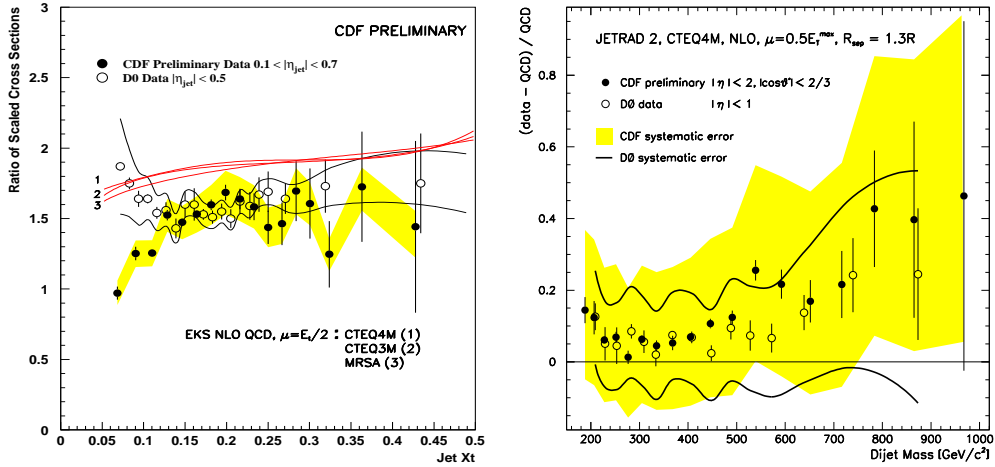


**FIGURE 4.** (a) Ratio of scaled cross sections ( $\sqrt{s} = 630 \text{ GeV}/\sqrt{s} = 1800 \text{ GeV}$ ) compared to an NLO calculation with three proton PDF's. (b) Relative difference of dijet invariant mass, measured by CDF and D0, compared with an NLO prediction (from [11]).

Consideration of the invariant mass of the dijet system, like the inclusive jet cross section, provides both a test of QCD and the opportunity to search for new physics. Figure 4b shows the comparison of both experiments, CDF and D0, with an NLO prediction, where the two measurements are defined with jets in different angular regions. The measured data agree very well between experiments and with the theory. There is a tendency for the data to deviate from the prediction at high masses, but the systematic errors are too large to make any firm conclusions.

## Jet substructure

Jet substructure has been studied at the Tevatron by considering both the jet shape and subjet multiplicity. Rerunning the  $k_T$  algorithm on those particles as-

signed to jets and stopping the clustering when all values of  $d_{ij}$  satisfy  $d_{ij} > y_{\text{cut}} E_T^2$  gives numbers of subjets as a function of  $y_{\text{cut}}$ . Figure 5 show two different measurements of subjets using the  $k_T$  algorithm [12,13], where Figure 5a shows a comparison of the number of subjets in data and different MC's and Figure 5b shows how the subjet multiplicity can be used to differentiate between quark and gluon jets. The jets measured in Figure 5a are above 250 GeV, which means that the scale being studied at the lowest  $y_{\text{cut}}$  is about 1 GeV. When one considers this range in scale, the description of the data by HERWIG is extremely good. Figure 5b demonstrates a method for separating quark and gluon jets based on a statistical subtraction for events at  $\sqrt{s} = 630$  GeV and  $\sqrt{s} = 1800$  GeV. As expected, gluon jets show more activity than quark jets. A method for distinguishing quark and gluon jets has also been developed by the ZEUS collaboration [8].

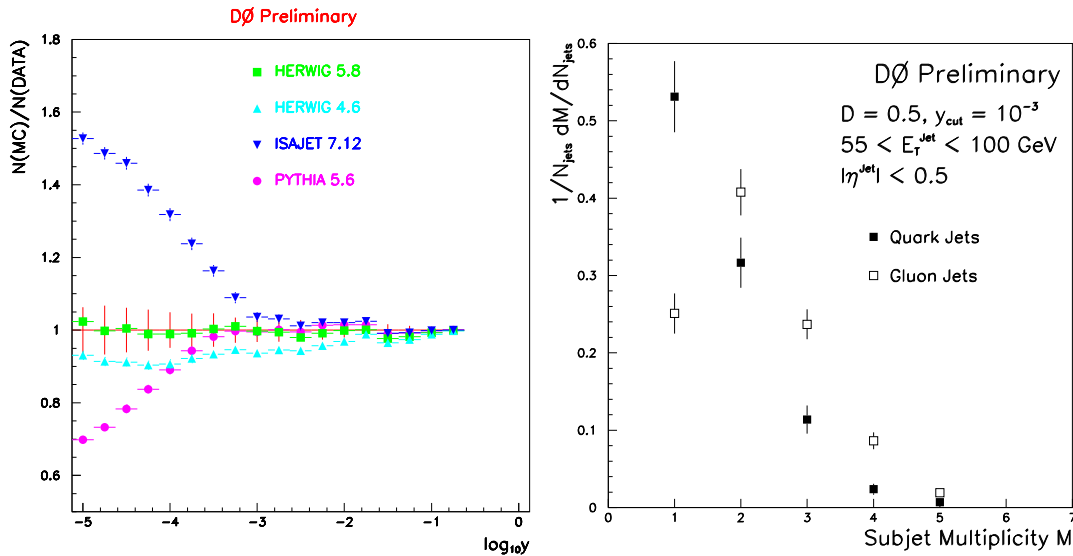


**FIGURE 5.** (a) Ratio of the multiplicity of subjets for data and MC for  $E_T^{\text{jet}} > 250$  GeV (from [12]). (b) Corrected subjet multiplicity in  $q$  and  $g$  jets extracted from D0 data (from [13]).

## Prompt photon production

Extensive measurements have been made and much theoretical work performed on prompt photon production at the Tevatron and fixed target experiments. Standard NLO perturbative calculations are unable to adequately describe the data at the Tevatron as shown in Figure 6a. Here, it can be seen that the data rise dramatically at low  $-p_T$ , the shape of which cannot be reproduced with a simple variation of the scale. The data can be described, however, by including an “intrinsic  $k_T$ ” for the partons in the proton. Figure 6b shows the calculation rising at low  $-p_T$  when a value of  $\langle k_T \rangle = 3.5$  GeV is used [14]. The use of intrinsic  $k_T$  is somewhat unsatisfactory, differing between data sets and centre-of-mass energies.

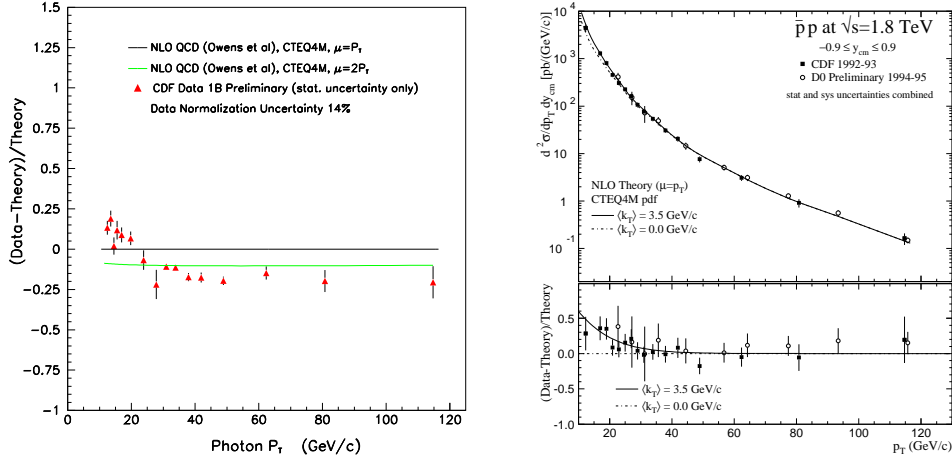


**FIGURE 6.** (a) CDF prompt photon production data compared to NLO predictions (from [11]). (b) CDF and D0 data compared to NLO predictions with intrinsic  $k_T$  and a value of  $\langle k_T \rangle = 3.5$  GeV (from [14]).

Prompt photon production has been extensively measured in fixed target experiments which have been compared with NLO predictions [15]. The NLO calculation from Aurenche et al [15] is able to describe all the fixed target data above a cut-off,  $E_T \geq 4 - 5$  GeV except that from E706. The ratio of data to theory is shown in Figure 7a, where the E706 data is shown to dramatically rise at low  $x_T = 2p_T/\sqrt{s}$ .

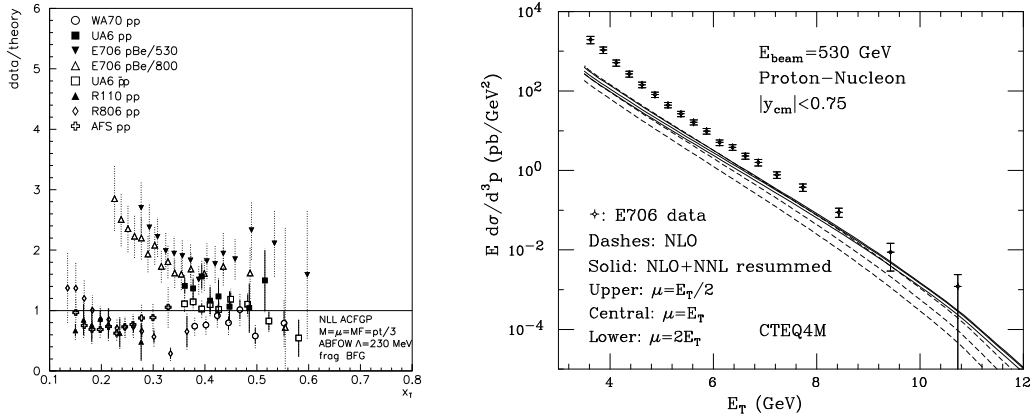


**FIGURE 7.** (a) Fixed target prompt photon data compared to NLO (from [15]). (b) Data from E706 compared to NLO predictions which have resummed large logarithms in  $x_T$  (from [16]).

Calculations resumming large logarithms in  $x_T$  [16] are also unable to describe the E706 data as shown in Figure 7b, although one would expect the resummation to improve the high- $p_T$  and not low- $p_T$  region. Figure 7b also demonstrates how

the resummation reduces the scale uncertainty in the calculation. Calculations in which  $Q_T$ , the nett transverse momentum of the final state  $\gamma q$  pair, is resummed [17] improve the description of the E706 data at low  $p_T$ , although the NLO prediction is still too low. HERA data can provide useful information on intrinsic  $k_T$ , by filling the energy “gap” between the fixed target and Tevatron experiments [7].

## HIGHER ORDER CALCULATIONS

The last few years have seen large advances in producing higher order calculations for the production of two or three jets [18,19]. Calculations of NLO 3–jet hadroproduction are becoming available and NNLO 2–jet hadroproduction will be produced sometime in the future. The needs for a 3–jet NLO calculation are many [18]. Measuring the 3–jet to 2–jet production ratio and hence  $\alpha_s$  will be possible with a 3–jet NLO calculation. As well as testing QCD, the calculation will provide a better understanding of backgrounds to new physics processes. It is also an important step towards calculating NNLO 2–jet production.

Figure 8 shows the predicted cross section for the highest-transverse-energy jet in 3–jet hadroproduction for both LO and NLO and their respective estimations of the scale uncertainty. The central NLO and LO predictions are of similar value, however, NLO shows a large reduction in the scale uncertainty over LO.

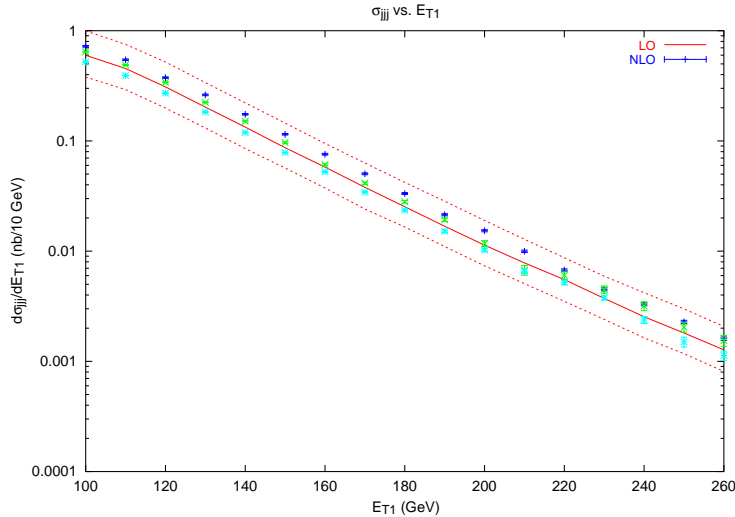


**FIGURE 8.** Predicted cross section for the highest-transverse-energy jet for 3–jet hadroproduction ( $\sqrt{s} = 1800$  GeV) where,  $E_T^{\text{jet}1} > 100$  GeV,  $E_T^{\text{jet}2,3} > 50$  GeV and  $|\eta^{\text{jet}}| < 4$ . The LO prediction with an estimation of the scale uncertainty is given by the lines and the NLO prediction with the corresponding estimation of the scale uncertainty is given by the points (from [18]).

Progress on calculations of NNLO 2–jet hadroproduction has been good over the last two years and the interested reader is referred to recent talks on the subject [19].

A NNLO calculation for the production of two jets is anticipated in a few years where a reliable estimate of the error on the cross section will be achieved.

## CONCLUSIONS

From the results presented, it can be seen that the theory of pQCD broadly describes the theory of the strong interaction. However, more detail both experimentally and theoretically is required to test QCD to great precision. This can also be achieved by considering the information from all experiments and what their results mean for each other.

## REFERENCES

1. ZEUS Collab., J.Breitweg et al., *Euro. Phys. J.* **C11**, 427 (1999).
2. Frixione, S., *Nucl. Phys. B* **507**, 295 (1997); Frixione, S. and Ridolfi G., *Nucl. Phys. B* **507**, 315 (1997); Harris, B., Klasen M. and Vossebeld, J. [hep-ph/9905348](#); Pötter B., [hep-ph/9911221](#).
3. Aurenche, P., et al., [hep-ph/0006011](#).
4. H1 Collab., H1prelim-00-052, Submitted to ICHEP2000 , Osaka, Japan.  
[www-h1.desy.de/h1/www/publications/htmlsplit/H1prelim-00-052.long.html](#)
5. ZEUS Collab., ICHEP-418, Submitted to ICHEP2000 , Osaka, Japan.  
[http://www-zeus.desy.de/~schlenst/conf/osaka\\_paper/QCD/dijetpho.ps.gz](#);  
ZEUS Collab., EPS - 540, Submitted to the EPS High Energy Physics 99 conference, Tampere, Finland. [http://www-zeus.desy.de/eps99/eps99\\_540.ps.gz](#)
6. Surow, B., (these proceedings)
7. Terron, J., (these proceedings)
8. Glasman, C. (these proceedings)
9. CDF Collab., *Phys. Rev. Lett.* **77** 438.
10. D0 Collab., *Phys. Rev. Lett.* **82** (1999) 2451.
11. [http://www-cdf.fnal.gov/physics/new/qcd/qcd99\\_blessed\\_plots.html](#)
12. R. V. Astur, Proc. 10th Topical Workshop on Proton-Antiproton Collider Physics, 1995, eds. R. Raja and J. Yoh, p. 598.
13. D0 Collab., [hep-ex/9907059](#), Submitted to the International Europhysics Conference on High Energy Physics, Tampere, Finland.
14. Apanasevich, L., et al., *Phys. Rev.* **D59** (1999) 074007.
15. Aurenche, P., et al., *Euro Phys. J.* **C9** (1999) 107.
16. Catani, S., et al., *JHEP* **9903** (1999) 25.
17. Laenen, E., Sterman, G. and Vogelsang, W., [hep-ph/0006352](#) To appear in DIS2000 conference proceedings.
18. Kilgore, W. and Giele, W., “Hadronic three jet production at NLO”, Talk presented at ICHEP2000, Osaka, Japan.
19. Glover, N., “Jet cross sections in NLO QCD and beyond”, Talk presented at DIS2000, Liverpool, UK; Bern, Z., Dixon, L. and Kosower, D. “Recent progress in NNLO QCD calculation”, Talk presented at ICHEP2000, Osaka, Japan.